

RESEARCH ARTICLE | MARCH 17 2025

Adaptive kink filtration: Achieving asymptotic size-independence of path integral simulations utilizing the locality of interactions

Amartya Bose  



J. Chem. Phys. 162, 114105 (2025)

<https://doi.org/10.1063/5.0256855>



Articles You May Be Interested In

QuantumDynamics.jl: A modular approach to simulations of dynamics of open quantum systems

J. Chem. Phys. (May 2023)

Quantum correlation functions through tensor network path integral

J. Chem. Phys. (December 2023)

A multisite decomposition of the tensor network path integrals

J. Chem. Phys. (January 2022)

Adaptive kink filtration: Achieving asymptotic size-independence of path integral simulations utilizing the locality of interactions

Cite as: J. Chem. Phys. 162, 114105 (2025); doi: 10.1063/5.0256855

Submitted: 7 January 2025 • Accepted: 24 February 2025 •

Published Online: 17 March 2025



View Online



Export Citation



CrossMark

Amartya Bose^{a)} 

AFFILIATIONS

Department of Chemical Sciences, Tata Institute of Fundamental Research, Mumbai 400005, India

^{a)}Author to whom correspondence should be addressed: amartya.bose@tifr.res.in

ABSTRACT

Recent method developments involving path integral simulations have come a long way in making these techniques practical for studying condensed phase non-equilibrium phenomena. One of the main difficulties that still needs to be surmounted is the scaling of the algorithms with the system dimensionality. The majority of recent techniques have only changed the order of this scaling (going from exponential to possibly a very high-ordered polynomial) and not eased the dependence on the system size. In this current work, we introduce an adaptive kink filtration technique for the path generation approach that leverages the locality of the interactions present in the system and the consequent sparsity of the propagator matrix to remove the asymptotic size dependence of the simulations for the propagation of reduced density matrices. This enables the simulation of larger systems at a significantly reduced cost. This technique can be used for simulation of both non-equilibrium dynamics and equilibrium correlation functions and is demonstrated here using examples from both. We show that the cost becomes constant with the dimensionality of the system. The only place where a system size-dependence still remains is the calculation of the dynamical maps or propagators, which are important for the transfer tensor method. The cost of calculating this solvent-renormalized propagator is the same as the cost of propagating all the elements of the reduced density matrix, which scales as the square of the size. This adaptive kink-filtration technique promises to be instrumental in extending the affordability of path integral simulations for very large systems.

Published under an exclusive license by AIP Publishing. <https://doi.org/10.1063/5.0256855>

I. INTRODUCTION

Simulation of the dynamics of open quantum systems has been a perpetual challenge owing to the exponential growth of computational complexity of quantum dynamics with the number of degrees of freedom. Avoiding this “curse of dimensionality” and side-stepping the exponential scaling have become a cornerstone of method development in the field. The relevance of such efforts is amply illustrated by the relevance of these simulations in the world of artificial photosynthesis and quantum computing. While wave function propagation approaches such as the density matrix renormalization group (DMRG)¹ and its time-dependent variant (t-DMRG)^{2,3} and the (multilevel) multiconfiguration time-dependent Hartree [(ML)-MCTDH]^{4–6} are capable of handling large systems, they are still not able to handle a continuum of environment degrees of freedom populated at finite temperatures efficiently.

A lucrative alternative to wave function-based methods is methods that simulate the dynamics of the reduced density matrix.

While approximate methods such as the Bloch–Redfield master equation, the Lindblad master equation, and multichromophoric incoherent Förster theory are commonly used in different circumstances, path integrals offer a way to simulate the dynamics in a numerically rigorous manner incorporating the effects of the dissipative media without any approximation using the Feynman–Vernon influence functional.⁷ The quasi-adiabatic propagator path integral^{8–10} (QuAPI) family of methods and the hierarchical equations of motion^{11,12} (HEOM) family of methods form two of the most commonly used frameworks that allow for such calculations. HEOM has historically been limited to using a Drude–Lorentz description of the dissipative environment. A flurry of recent work, though, has been geared toward expanding the capabilities of the original algorithm to dealing with non-Drude–Lorentz baths and especially more structured environments.^{13–18}

While these numerically rigorous path integral methods are capable of giving the correct dynamics irrespective of the coupling

involved, the cost of the calculations grows exponentially with the system size within the non-Markovian memory length. The transfer tensor method (TTM)¹⁹ and the small matrix decomposition of path integrals (SMatPIs)²⁰ alleviate the cost of propagating the reduced density matrix beyond the memory length. A different set of methods have been aimed at addressing the simulation within the memory length, which can then be leveraged by the previous two methods to simulate beyond it. This intrinsically non-Markovian portion of the dynamics proves to be more challenging to handle. While the blip decomposition^{21,22} was used to bring down the cost based on the structure of the influence functional, various methods based on tensor networks^{23–26} utilize the relative locality of the non-Markovian memory to improve the scaling of the full path simulations. Furthermore, the multi-site tensor network path integral approach²⁷ has used tensor networks to capitalize the short-ranged nature of the interactions between various units of a long aggregate to improve the performance of path integrals for extended systems. These methods have made the application of path integrals to large molecular aggregates increasingly approachable.²⁸ All of these tensor network-based methods bring down the exponential scaling of the algorithm to some polynomial scaling.

However, one of the important problems that remain is how to tackle larger systems. The cost of the full-path simulation grows extremely rapidly with the system size. Recently, Makri has shown that limiting the number of kinks (or time steps where the state of the system changes in a given path) allowed in the paths proves to be an interesting alternative approach to building the path list for the simulations.²⁹ While it is also able to curb the exponential scaling to a polynomial algorithm, this kink-summed path integral approach still scales as a high-degree polynomial of the size of the system. Here, it should be mentioned that the modular path integral (MPI)³⁰ and the multi-site tensor network path integral (MS-TNPI)²⁷ are capable of handling large systems with relatively local interactions.

In this paper, we ask if it is possible to reduce the complexity of path integrals for extremely large systems. The dream is to attempt to ensure that for very large systems, asymptotically, the scaling of the path integral becomes a constant instead of depending on the system size. A crucial step toward this goal is in the identification of the fact that even in the presence of long-ranged interactions, for all physical systems, the extent of these long-ranged interactions is much smaller than the size of the aggregates. As a result, the system propagators become sparse. This current work leverages the sparsity of the propagator matrix in developing a path filtration technique in which the number of paths does not scale with the system size beyond some threshold size. The kink filtration technique developed here additionally does not depend on particular structures of the Hamiltonian. This paper is organized as follows: in Sec. II, we motivate the method by exploring some simple closed-system problems. The path generation algorithm is developed using these intuitions. Then, in Sec. III, we apply this algorithm to study the non-equilibrium excitonic dynamics of a chain of bacteriochlorophyll molecules and simulate equilibrium correlation functions of open quantum systems; finally, we end this paper with some concluding remarks. The algorithms are implemented as a part of the `QuantumDynamics.jl` framework.³¹

II. MOTIVATION AND METHOD

Before including the thermal dissipative environment, let us start by analyzing a discretized path integral representation of the wave function propagation for a system defined by the Hamiltonian

$$\hat{H}_0 = \epsilon \sum_{j=1}^d |j\rangle\langle j| + \sum_{j>k} J(|j-k|)(|j\rangle\langle k| + |k\rangle\langle j|). \quad (1)$$

This is a simple Frenkel-like model for exciton or charge transport with d sites. The state $|k\rangle$ represents the excitation (or charge) on the k th molecule or site and every other site in the ground (or neutral) states and spans a d -dimensional Hilbert space. The electronic coupling between two states, $|j\rangle$ and $|k\rangle$, is given by some function J of the distance between the two sites. Typically, the physics of dipolar interactions implies that J would decay with distance (as R^{-3} , where R is the distance, but we do not make that assumption for the ensuing discussion).

If we start from an initial state $|\psi(0)\rangle$, then the time propagated wave function is given as follows:

$$\langle s_N | \psi(N\Delta t) \rangle = \prod_{j=0}^{N-1} \sum_{s_j} \langle s_{j+1} | \hat{U}_\Delta | s_j \rangle \langle s_0 | \psi(0) \rangle, \quad (2)$$

where

$$\hat{U}_\Delta = \exp\left(-i \frac{\hat{H}_0 \Delta t}{\hbar}\right). \quad (3)$$

Here, $\{s_j\}$ is the path under consideration connecting the initial state at s_0 to the final state at s_N in N time steps. If the dimensionality of the Hilbert space is d , then this scales as $\mathcal{O}(d^N)$ as every point in the path, s_j , is d -dimensioned. The recently developed kink-summed path integral²⁹ groups the paths in terms of the number of kinks it possesses, where a kink is defined as a segment where $s_j \neq s_{j+1}$. Makri has recently showed²⁹ that while the number of paths with a particular number of kinks undergoes a maximum at $\frac{N}{2}$, the net amplitude contributed by the set of paths with a particular number of kinks first increases and then decreases becoming practically negligible by the time one incorporates 8–9 kinks. Hence, in condensed phase simulations, it may not be necessary to include all kinks to get the correct dynamics.

To understand the complexity of a kink-summed path integral wave function simulation, one needs to count the number of N -time step paths involving up to K . This is given by

$$\sum_{k=0}^{\min(N,K)} \binom{N}{k} (d-1)^k. \quad (4)$$

If all kinks are accounted for, this binomial expansion sums to be the expected d^N . The computational complexity of the kink-summed path integral on including up to K kinks is a polynomial of order K (for $N > K$). Surprisingly, if the number of blips that we need to incorporate is around 8 or 9, this cost asymptotically becomes significantly larger than the polynomial dependence of the tensor network algorithms.^{23,32}

The holy grail of the algorithm design, therefore, would be to attempt to remove the d -dependence of the computational

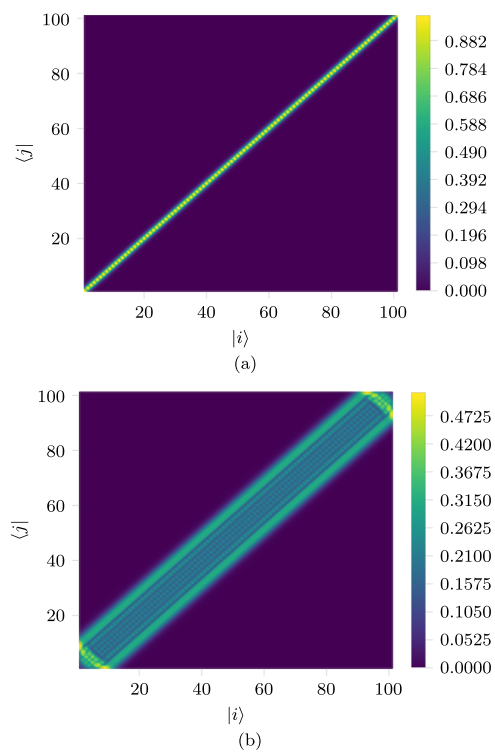


FIG. 1. Absolute value of short time propagators for the 101-mer Frenkel exciton model with $\epsilon = 0$, $J(R) = -\frac{1}{R^3}$ at two different values of Δt . (a) $\Delta t = 0.25$. (b) $\Delta t = 5.0$.

complexity. To that end, we note that because of the relatively short-ranged interactions present in the Hamiltonian (that is J decays with distance), the propagator ends up connecting “sites” that are relatively close as well. In Fig. 1, we plot the absolute values of all the elements of the short-time propagator for a long-distance interacting dipolar exciton-transfer model with 101 sites or $d = 101$. The propagators are calculated at $\Delta t = 0.25$ and $\Delta t = 5.0$. For the isolated system, the propagation is exact at all values of Δt . However, as soon as we put in the environment, the system–environment coupling would put an upper bound on the size of Δt that is converged due to errors associated with Trotter splitting of the propagator. Notice that the propagator is almost completely diagonal at the shorter values of Δt , despite having a long-range coupling $J(R) = -\frac{1}{R^3}$. This can be understood quite simply by expanding Eq. (3),

$$\hat{U}_\Delta = \mathbb{I} - i \frac{\hat{H}_0 \Delta t}{\hbar} + \mathcal{O}\left(\left(\frac{H \Delta t}{\hbar}\right)^2\right). \quad (5)$$

Therefore, at very short times, the structure and the sparsity of the propagator matrix are the same as those of the Hamiltonian. Hence, of the $d - 1$ possible kink segments, only a very few of them would contribute a non-negligible amplitude as long as Δt is relatively small. Even at significantly larger times, we notice that the propagator, while not diagonal, still has a band structure and is quite sparse. The breadth of this band is related to the maximum value of $|i - j|$ for which $\langle i | \hat{U}_\Delta | j \rangle$ has a non-negligible contribution. This determines the number of kinks that are relevant to the calculation.

A. Path generation algorithm

The goal, then, is to design an approach to path generation that leverages the relative locality of interaction and the consequent sparsity of the propagator matrix to generate the optimal path list. This should allow us to achieve asymptotic size-independence for the path integral simulations while being able to take advantage of the latest developments that have made simulations significantly more feasible. Consider the following algorithm of generating paths of N time steps with a maximum of K blips:

1. Start with the set of all $N - 1$ time step paths with K or less blips, S_K^{N-1} .
2. For every path in S_K^{N-1} , create N time step paths by repeating the last element in the path. These would constitute the paths that do not have a kink on the final segment.
3. For all paths in S_K^{N-1} with less than K kinks, create N time step paths by conditionally appending an element that is not the final element of the path. The condition is that if $l \neq p_{N-1}$ is the state that is being considered for extending the path and p_{N-1} is the final element of the path p in S_K^{N-1} , then $|\langle l | U_\Delta | p_{N-1} \rangle| \geq \chi |\langle p_{N-1} | U_\Delta | p_{N-1} \rangle|$, where χ is some user-defined threshold.

Starting with all possible paths for $N = 0$ time steps, the above three steps give us an inductive algorithm for generating the path lists for all other N 's and K 's. To clarify the goal of the path generation algorithm further, assume that we are not putting an upper limit on the number of blips. Then the path list that is generated would still not contain all possible kink transitions. Only those kink transitions would be allowed whose amplitude is higher than the cutoff, χ . This is the idea behind the adaptive kink-filtration. In terms of Fig. 1, we are trying to restrict our propagator to only allow for kinks within the central band where the propagator matrix elements are non-negligible. The value of χ is used as a convergence parameter and systematically decreased till convergence. In a similar vein, the number of permissible kinks would be increased till convergence. Notice that neither of these is an *ad hoc* approximation and can be systematically relaxed till convergence. In this way, we can generate an adaptive path list, which reflects the structure of the system Hamiltonian while remaining compatible with the kink-summation ideas.²⁹

Before launching into examples of open quantum systems, first as an instructive exercise, let us see what kind of impact this adaptive kink-filtration has on wave-function propagation of bare excitonic systems. Consider the 101-mer long nearest-neighbor interacting Frenkel chain, with $\epsilon = 0$ and $J(R) = 1.0$ if $R = 1$ and $J(R) = 0.0$ otherwise; we show a comparison between the analytical dynamics of the middle site and the number of paths involved in Fig. 2. A cut-off of $\chi = 0.01$ is sufficient in converging the dynamics up to $\Delta t = 3$. Paths with all kinks were considered in this illustrative simulation. A naïve full path calculation would use 101^N paths for an N time step calculation. Whereas with $\chi = 0.1$, we get a scaling of 3^N , at $\chi = 0.01$, the scaling increases to 7^N . It is obvious that the filtration is extremely consequential in lowering the number of paths. In fact, using the adaptive algorithm outlined here, the full path list is never even generated. It should be reiterated that the goal of the method is not to simulate isolated systems, where the results can be obtained trivially, but to enable simulations of condensed phase systems using a scheme that allows for systematic convergence as demonstrated in

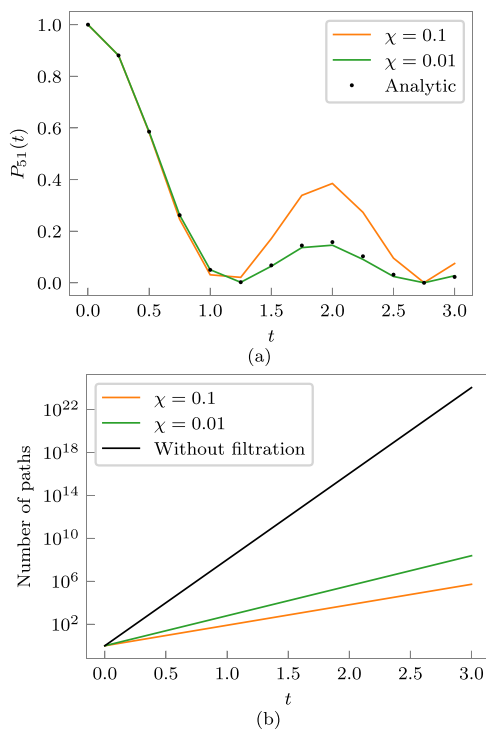


FIG. 2. Survival probability of the middle monomer of a nearest-neighbor interacting aggregate with 101 monomers at two different values of the filtration cutoff χ and the corresponding number of paths. (a) Dynamics. (b) Number of paths.

Sec. III. This illustration was just provided to establish the intuition behind the scheme.

To further investigate the effect of system size on the number of filtered kink paths, let us consider linear aggregates of sizes from 2 (dimer) to 100 with either a nearest neighbor coupling of $J = -1$ or the long ranged coupling of $J(R) = -R^{-3}$. In Fig. 3, we show the number of paths as a function of the system size. Notice that in both cases, when filtered with $\epsilon = 0.01$, the number of paths included in an eight-kink calculation of ten time step paths very quickly reaches a constant number. This constant number is, of

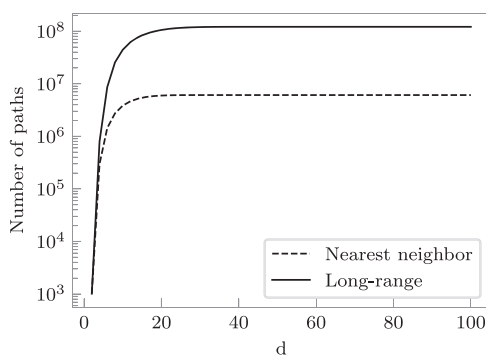


FIG. 3. Number of paths vs system size, d , for an eight-kink calculation out to ten time steps for a threshold of $\epsilon = 0.01$.

course, dependent upon the sort of interaction present in the system. For the nearest-neighbor interacting system, the number is significantly smaller than the long-range interacting system. This is in contrast to the unfiltered eight-kink paths that will continue to grow as $\mathcal{O}(d^8)$ irrespective of the type of interactions present in the system. Thus, by utilizing the local nature of the short-time propagator, one can make path integrals scale independently of the system size for asymptotically large systems.

One can, in principle, have other distance dependencies of the Hamiltonian. Most commonly, $J(R) \sim R^{-1}$ for unshielded Coulomb interactions, and for polaritonic systems, the coupling with the cavity mode would not have any decay with “distance,” which is an ill-defined concept in the context of cavity coupling. Let us discuss these two common cases before moving on to the simulation of open quantum systems. In the first case of the Coulomb interactions, one can still see a potentially slow fall-off of the interaction. The path generation algorithm outlined in this section uses cutoffs to eliminate the propagator matrix elements. The cutoff can be systematically reduced till convergence is attained. Therefore, for Coulomb interactions, the asymptotically constant size of the path list would be slower to set in in comparison to the dipolar interactions or say to the nearest neighbor interactions in the limiting case. For the second case of interactions with the cavity mode, it is a single “site” that does not follow the physics of decay of interactions. Hence, the algorithm would still provide enormous benefits to the computation while ensuring that the cavity coupling to all the monomers is still incorporated correctly.

Finally, there are other types of geometries that need to be considered. Suppose instead of a chain, the system under study has a ring topology. In that case, the only extra thing that needs to be considered is the connection between the “ends” of the chain. The adaptive nature of the kink-filtration algorithm keeps these particular connections alive while removing the other unimportant couplings. The entire physics is captured by the propagator matrix elements and the structure thereof. The kink-filtration procedure removes only the elements that are less important than a user-defined cutoff and can consequently handle arbitrary structures. In the limiting case of every site being equally coupled with every other site, the adaptive kink-filtration would not be able to achieve any extra speed up and the cost of calculation is the same as the usual path integral simulation. In this sense, the method outlined here is not an *ad hoc* approximation and can systematically be converged for all cases.

Next, in Sec. III, we will incorporate this path generation algorithm in simulations of open quantum systems with Feynman–Vernon influence functionals.⁷ Our applications will range from simulations of non-equilibrium dynamics to equilibrium correlation functions in the context of spectra. In each case, the use of the path generation algorithm is slightly different and would be developed separately in the discussion.

III. NUMERICAL EXAMPLES OF OPEN QUANTUM SYSTEM

Till now, we explored the idea in the context of wave function dynamics of isolated systems. Most systems of interest are not actually isolated and interact with thermal environments. In such cases, the effect of the environment needs to be accounted for. The

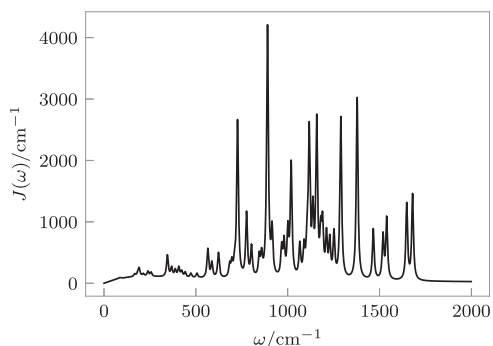


FIG. 4. Spectral density for the bacteriochlorophyll molecule.

Hamiltonian describing such a system–environment coupled problem is generally expressed as follows:

$$\hat{H} = \hat{H}_0 + \hat{H}_{\text{sys-env}}, \quad (6)$$

where \hat{H}_0 is the system Hamiltonian and $\hat{H}_{\text{sys-env}}$ accounts for the environment and the interaction terms. Under Gaussian response, the molecular environment can often be mapped on to one or more baths of harmonic oscillators,

$$\hat{H}_{\text{sys-env}} = \sum_{b=1}^{N_b} \sum_{j=1}^{N_{\text{osc}}} \frac{p_{bj}^2}{2} + \frac{1}{2} \omega_{bj}^2 \left(x_{bj} - \frac{c_{bj} \hat{s}_b}{\omega_{bj}^2} \right)^2. \quad (7)$$

Here, N_b is assumed to be the number of baths, each with N_{osc} oscillators. The b th bath interacts with the system through the operator, \hat{s}_b . For simplicity, it is also assumed that $[\hat{s}_{b_1}, \hat{s}_{b_2}] = 0$ for any $b_1 \neq b_2$. The frequency, ω_{bj} , and coupling, c_{bj} , of the j th mode of the b th bath are linked via the spectral density describing this bath,

$$J_b(\omega) = \frac{\pi}{2} \sum_j \frac{c_{bj}^2}{\omega_{bj}} \delta(\omega - \omega_{bj}). \quad (8)$$

The spectral density is crucially important to the dynamics and can be estimated from experiments³³ or simulations³⁴ or a mixture thereof. It is related to the energy-gap auto-correlation function.

As an example of an open quantum system consider a chain of nearest-neighbor interacting bacteriochlorophyll molecules. The electronic coupling is $J = -363 \text{ cm}^{-1}$. Every molecule is coupled to vibronic degrees of freedom, which are described by local harmonic baths. The spectral density, shown in Fig. 4, is the same as the one studied in Ref. 35. It is taken to be the sum of the 50 relevant rigid vibrations and their Huang–Rhys factors as reported by Rätsep *et al.*³³ and an unstructured Brownian portion with a reorganization energy of 109 cm^{-1} . The contribution of the rigid vibrations and their Huang–Rhys factors to the spectral density has been broadened using a Lorentzian of width 10.97 cm^{-1} .

A. Non-equilibrium dynamics using QuAPI

If the initial state does not have system–environment entanglement and the environment is in a thermal state, then $\rho(0) = \tilde{\rho}(0) \otimes \frac{\exp(-\beta H)}{Z_{\text{env}}}$; then, the dynamics of the reduced density matrix

corresponding to the system is given in the path integral formalism as follows:

$$\langle s_N^+ | \tilde{\rho}(N\Delta t) | s_N^- \rangle = \sum_{s_{N-1}^\pm} \sum_{s_{N-2}^\pm} \cdots \sum_{s_0^\pm} \langle s_N^+ | U_\Delta | s_{N-1}^+ \rangle \langle s_{N-1}^+ | U_\Delta | s_{N-2}^+ \rangle \times \cdots \langle s_1^+ | U_\Delta | s_0^+ \rangle \langle s_0^+ | \tilde{\rho}(0) | s_0^- \rangle \langle s_0^- | U_\Delta^\dagger | s_1^- \rangle \times \langle s_1^- | U_\Delta^\dagger | s_2^- \rangle \cdots \langle s_{N-1}^- | U_\Delta^\dagger | s_N^- \rangle \times F[s^\pm(t)], \quad (9)$$

where s_j^\pm are the forward–backward path points at the j th time step and F is the Feynman–Vernon influence functional⁷ and is related to the spectral density describing the solvent^{8,9} and the energy-gap correlation function.³⁶ This influence functional makes the dynamics non-Markovian, though in condensed phases the length of the memory caused by the environment is finite.

Notice that the path integral expression in Eq. (9) can be thought of as being composed of three parts, the amplitude of the forward path (s_0^+ to s_N^+), the amplitude of the backward path (s_0^- to s_N^-), and the influence functional corresponding to the forward–backward path ($F[s^\pm]$). Utilizing the path generation algorithm that we developed in Sec. II A, we can generate a kink-filtered forward path list and the corresponding bare amplitudes. Let this set be called S_f . The backward path list (called S_b) is identical but has amplitudes that are complex conjugates. These lists already utilize the sparsity of the bare system propagator. Now, the sum over the forward–backward paths is obtained by iterating over the set that is the Cartesian product of S_f and S_b . The bare amplitudes of the forward and backward paths are multiplied along with the influence functional. This full amplitude is finally added to get the density matrix according to Eq. (9).

However, because of the simplicity of the setup of doing path integral simulations using the adaptive kink-filtration algorithm, we can incorporate further enhancements through filtering by the absolute magnitude using a cutoff threshold³⁷ and finally by considering forward–backward paths with less than a particular number of blips.²¹ Blips are the time-points where the forward path differs from the backward paths. Each blip leads to an exponential decrease in the amplitude contributed by the path and has been successfully used to decompose the path sum, resulting in exponential speedups for some problems.^{21,22} Here, the number of blips is used as a mere means of

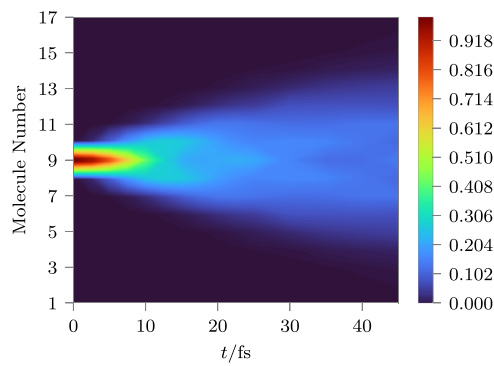


FIG. 5. Excitonic dynamics in a chain of 17 bacteriochlorophyll molecules at $T = 300 \text{ K}$.

path filtration to additionally enhance the efficiency of the simulations. This is done by considering only those forward and backward path pairs that differ at less than the permissible number of blips.

We demonstrate the full-memory simulation of the excitonic dynamics in a 17-mer chain of bacteriochlorophyll molecules at $T = 300$ K up to 40 fs using the adaptive kink filtration in Fig. 5. The initial condition is taken to be $\tilde{\rho}(0) = |9\rangle\langle 9|$, which is the middle monomer. The simulation used time steps of $\Delta t = 2.5$ fs summing up paths with at most nine kinks and ten blips till $t = 25$ fs; thereafter, it used a time step of $\Delta t = 5$ fs. As a demonstration of the effectiveness of the adaptive kink filtration method, the number of forward-backward paths summed for the tenth step of the simulation at $t = 50$ fs is shown in Fig. 6. Because the lines correspond to an eight-kink simulation, according to Eq. (4), the number of paths should go as an eight-power polynomial of the system size, d . However, notice that irrespective of the maximum number of blips considered, the number of paths saturates quite quickly. It becomes constant from around 12 monomers onward. While the exact number of paths would differ with cutoffs and the number of kinks and other factors, the trend of saturating with the number of monomers would be invariant.

These simulations are all done at full memory. There are currently three ways of going beyond this full memory regime: (1) traditional iteration techniques,^{8,9} (2) the transfer tensor method (TTM),¹⁹ or (3) the small matrix decomposition.²⁰ For concreteness, we discuss the iteration scheme using the TTM method in conjunction with the adaptive kink-filtered path integral. A TTM iteration starts with the computation of the dynamical map, $\mathcal{E}(t)$, within the memory length. This dynamical map connects the time-evolved reduced density matrix of the system to the initial condition, $\tilde{\rho}(t_n) = \mathcal{E}_n \tilde{\rho}(0)$. By comparing the definition of the dynamical map with the path integral expression [Eq. (9)], we notice that the dynamical map can be written as follows:

$$\langle s_N^\pm | \mathcal{E}_N | s_0^\pm \rangle = \sum_{s_{N-1}^\pm} \sum_{s_{N-2}^\pm} \cdots \sum_{s_1^\pm} \langle s_N^+ | U_\Delta | s_{N-1}^+ \rangle \\ \times \langle s_{N-1}^+ | U_\Delta | s_{N-2}^+ \rangle \cdots \langle s_1^+ | U_\Delta | s_0^+ \rangle \\ \times \langle s_0^- | U_\Delta^\dagger | s_1^- \rangle \langle s_1^- | U_\Delta^\dagger | s_2^- \rangle \cdots \\ \times \langle s_{N-1}^- | U_\Delta^\dagger | s_N^- \rangle \times F[s^\pm(t)]. \quad (10)$$

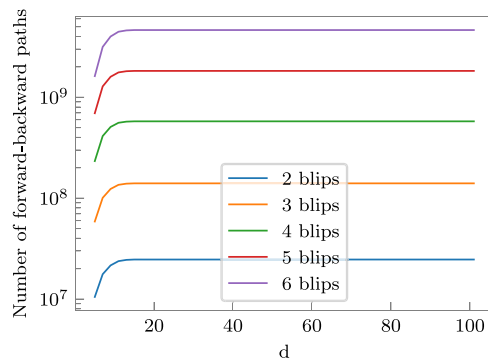


FIG. 6. Number of paths at $t = 50$ fs as a function of size of system, d , for a simulation with 8 kinks at $\Delta t = 5$ fs, $\chi = 0.01$, and a total amplitude cutoff of 10^{-8} .

This can be easily simulated using the adaptive kink-filtered path integral method within memory length (say, N_{mem} time steps) yielding transfer tensors¹⁹

$$T_n = \mathcal{E}_n - \sum_{j=1}^{n-1} T_{n-j} \mathcal{E}_j, \quad (11)$$

which capture the non-Markovianity of the dynamics and using which the reduced density matrix can be propagated beyond the memory length,^{19,31,38}

$$\tilde{\rho}(N\Delta t) = \sum_{k=1}^{N_{\text{mem}}} T_k \tilde{\rho}((N-k)\Delta t). \quad (12)$$

For a system of size d , this necessitates d^2 path integral calculations, each corresponding to a distinct choice of s_0^\pm in Eq. (10). Consequently, even though the number of paths in a single path integral calculation saturates to a constant value as $d \rightarrow \infty$, the number of paths required to obtain the dynamical map would asymptotically go as $\mathcal{O}(d^2)$.

B. Equilibrium correlation functions

Finally, this adaptive kink filtration is not just limited to the simulation of non-equilibrium dynamics. Its ability to generate an optimal set of paths for a given system can be directly utilized in improving the efficiency of the calculation of correlation functions as well. For illustration, we will concentrate on absorption and emission spectra of molecular aggregates. Consider a thermal quantum correlation function,

$$C_{AB}(t) \propto \text{Tr}(\hat{B}(t)\hat{A}(0)\exp(-\beta\hat{H})), \quad (13)$$

where \hat{A} and \hat{B} are the relevant system operators. For an absorption spectrum, $\hat{A} = \hat{\mu}_+$, which is the excitation operator, and $\hat{B} = \hat{\mu}_-$, which is the de-excitation operator. However, in the case of an emission spectrum, the operators are reversed ($\hat{A} = \hat{\mu}_-$ and $\hat{B} = \hat{\mu}_+$). The spectra are obtained as the Fourier transform of these correlation functions,³⁹

$$\sigma_{\text{abs}}(\omega) = \int C_{\mu_+\mu_-}(t) \exp(i\omega t) dt, \quad (14)$$

$$\sigma_{\text{ems}}(\omega) = \int C_{\mu_-\mu_+}(t) \exp(-i\omega t) dt. \quad (15)$$

Such correlation functions can be computed using the path integral formalism^{26,40} to account for the environment effects. Here, we adopt a complex time contour that is obtained by representing the correlation function in a way that combines the equilibrium density matrix with the backward propagator,

$$C_{AB}(t) \propto \text{Tr}\left(\exp\left(\frac{i\hat{H}t_c}{\hbar}\right)\hat{B}\exp\left(-\frac{i\hat{H}t}{\hbar}\right)\hat{A}\right), \quad (16)$$

where $t_c = t - i\beta\hbar$. (Notice that this definition of the complex-time differs from what is traditionally used when calculating symmetrized

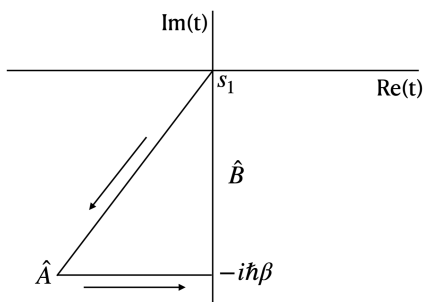


FIG. 7. Complex-time contour used for calculating the absorption and emission spectra. States s_1 to s_N are on the diagonal line and s_{N+1} to s_{N+2} are on the horizontal line connecting to the $t = -i\hbar\beta$ point.

complex-time correlation functions^{26,40} by a factor of 2 in the imaginary part. This contour in complex-time is shown in Fig. 7.) Consequently, the corresponding path integral becomes

$$\begin{aligned} C_{AB}(t) = & \sum_{s_1} \sum_{s_2} \cdots \sum_{s_{2N+2}} \langle s_1 | B | s_{2N+2} \rangle \langle s_{2N+2} | U_\Delta | s_{2N+1} \rangle \\ & \times \langle s_{2N+1} | U_\Delta | s_{2N} \rangle \dots \langle s_{N+2} | U_\Delta | s_{N+1} \rangle \langle s_{N+1} | \hat{A} | s_N \rangle \\ & \times \langle s_N | U_{\Delta c} | s_{N-1} \rangle \times \dots \times \langle s_3 | U_{\Delta c} | s_2 \rangle \langle s_2 | U_{\Delta c} | s_1 \rangle \times F_c[\{s_j\}], \end{aligned} \quad (17)$$

where

$$U_{\Delta c} = \exp \left(i\hat{H}_0 \frac{t}{N\hbar} - \hat{H}_0 \frac{\beta}{N} \right) \quad (18)$$

and

$$U_\Delta = \exp \left(-i\hat{H}_0 \frac{t}{N\hbar} \right). \quad (19)$$

Here, the influence functional, F_c , has been derived by Topaler and Makri⁴⁰ in terms of the spectral density and has a different form in comparison to the one used for real-time dynamics in Eq. (9). The paths along the complex-time contour, Fig. 7, are discretized as s_j .

In these cases, the adaptive kink procedure is trivially used to generate the sets of half-paths s_1 to s_{N+1} and s_{N+2} to s_{2N+2} using different short-time propagators $U_{\Delta c}$ and U_Δ , respectively. These can then be concatenated and used for obtaining the influence functional contributions. Because the complex-time propagators are further damped and consequently more sparse, we expect the efficiency of the adaptive kink filtration procedure to increase in comparison to the real time computation counterparts.

We simulate the absorption and emission spectra of bacteriochlorophyll chains of different sizes ranging from a dimer to a heptamer. The spectra are shown in Fig. 8. We notice a distinct red shift of both the emission and absorption line shapes with increasing system size before convergence to a particular location. The absorption line shape is significantly broader than the emission line shape in all cases. Its width also increases on going from a dimer to a trimer. Additionally, clearly visible from the plots is the Stoke's shift between the absorption and emission peaks, which is also size-dependent. For a dimer, it is around 167 cm^{-1} , and it increases to around 334 cm^{-1} .

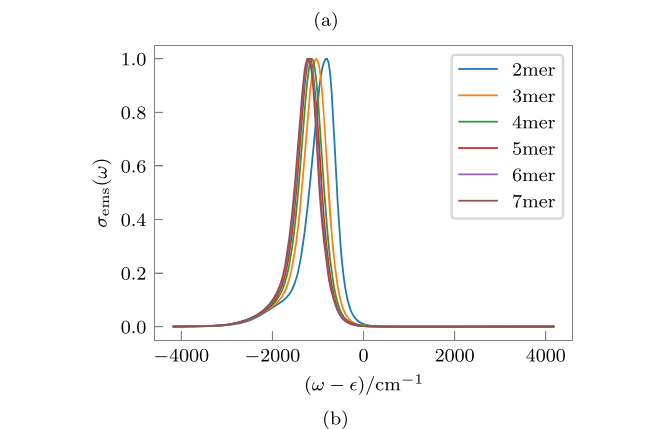
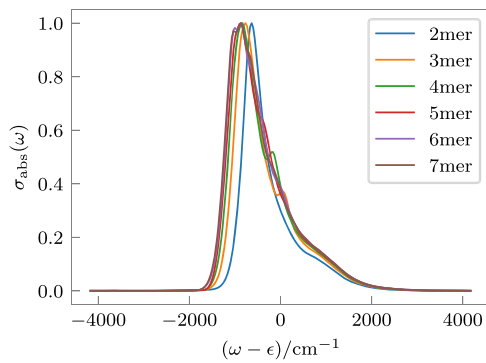


FIG. 8. Absorption and emission spectra of aggregates of different sizes. (a) Absorption spectrum. (b) Emission spectrum.

IV. CONCLUSION

In this paper, we have addressed the long-standing issue of the system size dependence of the computational complexity of path integral calculations. While in the recent times, much progress has happened in terms of reducing the scaling of the problem in terms of both the number of time steps and the size of the system, even the best of these methods scales as high powered polynomials of the system dimensionality. Thus, even with these developments, simulations are limited to relatively smallish cluster sizes. We design and present an adaptive kink filtration method that addresses this challenge, providing a first step of moving toward even larger systems.

In most physical systems, the interactions decay with distance, leading to relatively short-ranged interactions, which induce sparsity in the system propagator operator. We utilize this sparsity in developing an algorithm of path generation that ensures that the number of paths considered saturates after a certain system-dependence. The basic physical intuition is that in a large chain, sites that are separated by large distances should not be really coupled, and consequently, the amplitude for the system to hop between the said sites would be negligible. The adaptive kink filtration algorithm is a formalization of this simple intuition. Thus, asymptotically, the number of paths and therefore the complexity become a constant with the system size.

The adaptive kink filtration method does not assume any particular structure of the Hamiltonian as is assumed in the modular

path integral³⁰ or as is convenient for the multi-site tensor network path integral.²⁷ It simply creates a built-in adaptive algorithm that automatically generates only the most relevant paths to be added to the path list irrespective of the underlying structure of the system. The physics of the particular system Hamiltonian and the particular initial condition under study are automatically taken into account. In this sense, it is similar to other filtration algorithms. Additionally, this technique is fully compatible with existing techniques, such as magnitude-based^{37,41} and blip-based filtration²¹ and the kink sum²⁹ method.

In this work, we demonstrated the adaptive filtration technique by first studying the non-equilibrium exciton dynamics in a chain of bacteriochlorophyll molecules using the Feynman–Vernon influence functional. We showed the saturation of the number of paths as the number of molecules is increased. In addition to the adaptive kink filtration, we also used the path-based filtration³⁷ and blip filtration²¹ for additional efficiency.

Finally, we explore the possibility of using the adaptive kink-filtration to make simulations of correlation functions more efficient. To this end, we consider the absorption and emission spectra of excitonic aggregates in the presence of vibrations. In this case, the adaptive kink-filtration algorithm is used to generate the purely real-time and the complex-time halves of the path separately and then input into the path integral calculation. This demonstrates the versatility of the algorithm that stems from its simplicity.

Code implementing this algorithm has already been released in the *QuantumDynamics.jl*³¹ framework. The details of the use of the method in the code would be discussed in an upcoming publication along with examples. We believe that in conjunction with other recent developments oriented toward improving the scaling of path integral simulations, the adaptive kink-filtration technique outlined here would prove to be a key step in making simulations of large systems possible. A future study would focus on exciton-polaritonic systems among others because the almost uniform coupling of the molecules to the cavity mode provides an interesting case where the adaptive kink-filtration would prove to be super-efficient in going to large systems.

AUTHOR DECLARATIONS

Conflict of Interest

The author has no conflicts to disclose.

Author Contributions

Amartya Bose: Conceptualization (equal); Data curation (equal); Formal analysis (equal); Funding acquisition (equal); Investigation (equal); Methodology (equal); Project administration (equal); Resources (equal); Software (equal); Supervision (equal); Validation (equal); Visualization (equal); Writing – original draft (equal); Writing – review & editing (equal).

DATA AVAILABILITY

The data that support the findings of this study are available from the corresponding author upon reasonable request.

REFERENCES

- ¹S. R. White, “Density matrix formulation for quantum renormalization groups,” *Phys. Rev. Lett.* **69**, 2863–2866 (1992).
- ²S. R. White and A. E. Feiguin, “Real-time evolution using the density matrix renormalization group,” *Phys. Rev. Lett.* **93**, 076401 (2004).
- ³S. Paeckel, T. Köhler, A. Swoboda, S. R. Manmana, U. Schollwöck, and C. Hubig, “Time-evolution methods for matrix-product states,” *Ann. Phys.* **411**, 167998 (2019).
- ⁴H.-D. Meyer, U. Manthe, and L. Cederbaum, “The multi-configurational time-dependent Hartree approach,” *Chem. Phys. Lett.* **165**, 73–78 (1990).
- ⁵H. Wang and M. Thoss, “Multilayer formulation of the multiconfiguration time-dependent Hartree theory,” *J. Chem. Phys.* **119**, 1289–1299 (2003).
- ⁶H. Wang, “Multilayer multiconfiguration time-dependent Hartree theory,” *J. Phys. Chem. A* **119**, 7951–7965 (2015).
- ⁷R. P. Feynman and F. L. Vernon, “The theory of a general quantum system interacting with a linear dissipative system,” *Ann. Phys.* **24**, 118–173 (1963).
- ⁸N. Makri and D. E. Makarov, “Tensor propagator for iterative quantum time evolution of reduced density matrices. I. Theory,” *J. Chem. Phys.* **102**, 4600–4610 (1995).
- ⁹N. Makri and D. E. Makarov, “Tensor propagator for iterative quantum time evolution of reduced density matrices. II. Numerical methodology,” *J. Chem. Phys.* **102**, 4611–4618 (1995).
- ¹⁰N. Makri, E. Sim, D. E. Makarov, and M. Topaler, “Long-time quantum simulation of the primary charge separation in bacterial photosynthesis,” *Proc. Natl. Acad. Sci. U. S. A.* **93**, 3926–3931 (1996).
- ¹¹Y. Tanimura and P. G. Wolynes, “Quantum and classical Fokker-Planck equations for a Gaussian-Markovian noise bath,” *Phys. Rev. A* **43**, 4131–4142 (1991).
- ¹²Y. Tanimura, “Numerically ‘exact’ approach to open quantum dynamics: The hierarchical equations of motion (HEOM),” *J. Chem. Phys.* **153**, 20901 (2020).
- ¹³H. Rahman and U. Kleinekathöfer, “Chebyshev hierarchical equations of motion for systems with arbitrary spectral densities and temperatures,” *J. Chem. Phys.* **150**, 244104 (2019).
- ¹⁴T. Ikeda and G. D. Scholes, “Generalization of the hierarchical equations of motion theory for efficient calculations with arbitrary correlation functions,” *J. Chem. Phys.* **152**, 204101 (2020).
- ¹⁵Y. Yan, T. Xing, and Q. Shi, “A new method to improve the numerical stability of the hierarchical equations of motion for discrete harmonic oscillator modes,” *J. Chem. Phys.* **153**, 204109 (2020).
- ¹⁶Y. Yan, M. Xu, T. Li, and Q. Shi, “Efficient propagation of the hierarchical equations of motion using the Tucker and hierarchical Tucker tensors,” *J. Chem. Phys.* **154**, 194104 (2021).
- ¹⁷M. Xu, Y. Yan, Q. Shi, J. Ankerhold, and J. T. Stockburger, “Taming quantum noise for efficient low temperature simulations of open quantum systems,” *Phys. Rev. Lett.* **129**, 230601 (2022).
- ¹⁸Y. Ke, “Tree tensor network state approach for solving hierarchical equations of motion,” *J. Chem. Phys.* **158**, 211102 (2023).
- ¹⁹J. Cerrillo and J. Cao, “Non-Markovian dynamical maps: Numerical processing of open quantum trajectories,” *Phys. Rev. Lett.* **112**, 110401 (2014).
- ²⁰N. Makri, “Small matrix disentanglement of the path integral: Overcoming the exponential tensor scaling with memory length,” *J. Chem. Phys.* **152**, 41104 (2020).
- ²¹N. Makri, “Blip decomposition of the path integral: Exponential acceleration of real-time calculations on quantum dissipative systems,” *J. Chem. Phys.* **141**, 134117 (2014).
- ²²N. Makri, “Iterative blip-summed path integral for quantum dynamics in strongly dissipative environments,” *J. Chem. Phys.* **146**, 134101 (2017).
- ²³A. Strathearn, P. Kirton, D. Kilda, J. Keeling, and B. W. Lovett, “Efficient non-Markovian quantum dynamics using time-evolving matrix product operators,” *Nat. Commun.* **9**, 3322 (2018).
- ²⁴M. R. Jørgensen and F. A. Pollock, “Exploiting the causal tensor network structure of quantum processes to efficiently simulate non-Markovian path integrals,” *Phys. Rev. Lett.* **123**, 240602 (2019).

- ²⁵A. Bose, “Pairwise connected tensor network representation of path integrals,” *Phys. Rev. B* **105**, 024309 (2022).
- ²⁶A. Bose, “Quantum correlation functions through tensor network path integral,” *J. Chem. Phys.* **159**, 214110 (2023).
- ²⁷A. Bose and P. L. Walters, “A multisite decomposition of the tensor network path integrals,” *J. Chem. Phys.* **156**, 024101 (2022).
- ²⁸A. Bose and P. L. Walters, “Tensor network path integral study of dynamics in B850 LH2 ring with atomistically derived vibrations,” *J. Chem. Theory Comput.* **18**, 4095–4108 (2022).
- ²⁹N. Makri, “Kink sum for long-memory small matrix path integral dynamics,” *J. Phys. Chem. B* **128**, 2469–2480 (2024).
- ³⁰N. Makri, “Modular path integral methodology for real-time quantum dynamics,” *J. Chem. Phys.* **149**, 214108 (2018).
- ³¹A. Bose, “QuantumDynamics.jl: A modular approach to simulations of dynamics of open quantum systems,” *J. Chem. Phys.* **158**, 204113 (2023).
- ³²A. Bose and P. L. Walters, “A tensor network representation of path integrals: Implementation and analysis,” *arXiv:2106.12523* (2021).
- ³³M. Rätsep, Z.-L. Cai, J. R. Reimers, and A. Freiberg, “Demonstration and interpretation of significant asymmetry in the low-resolution and high-resolution Q_y fluorescence and absorption spectra of bacteriochlorophyll *a*,” *J. Chem. Phys.* **134**, 24506 (2011).
- ³⁴C. Olbrich, J. Strümpfer, K. Schulten, and U. Kleinekathöfer, “Theory and simulation of the environmental effects on FMO electronic transitions,” *J. Phys. Chem. Lett.* **2**, 1771–1776 (2011).
- ³⁵D. Sharma and A. Bose, “Impact of loss mechanisms on linear spectra of excitonic and polaritonic aggregates,” *J. Chem. Theory Comput.* **20**, 9522–9532 (2024).
- ³⁶A. Bose, “Zero-cost corrections to influence functional coefficients from bath response functions,” *J. Chem. Phys.* **157**, 054107 (2022).
- ³⁷E. Sim and N. Makri, “Tensor propagator with weight-selected paths for quantum dissipative dynamics with long-memory kernels,” *Chem. Phys. Lett.* **249**, 224–230 (1996).
- ³⁸A. Bose, “Incorporation of empirical gain and loss mechanisms in open quantum systems through path integral Lindblad dynamics,” *J. Phys. Chem. Lett.* **15**, 3363–3368 (2024).
- ³⁹M. Buser, J. Cerrillo, G. Schaller, and J. Cao, “Initial system-environment correlations via the transfer-tensor method,” *Phys. Rev. A* **96**, 062122 (2017).
- ⁴⁰M. Topaler and N. Makri, “Quantum rates for a double well coupled to a dissipative bath: Accurate path integral results and comparison with approximate theories,” *J. Chem. Phys.* **101**, 7500–7519 (1994).
- ⁴¹E. Sim and N. Makri, “Filtered propagator functional for iterative dynamics of quantum dissipative systems,” *Comput. Phys. Commun.* **99**, 335–354 (1997).